Article

Artificial Oligopeptide Scaffolds for Stoichiometric Metal Binding

Brian P. Gilmartin, Kristi Ohr, Rebekah L. McLaughlin, Richard Koerner, and Mary Elizabeth Williams

J. Am. Chem. Soc., **2005**, 127 (26), 9546-9555• DOI: 10.1021/ja0510818 • Publication Date (Web): 14 June 2005

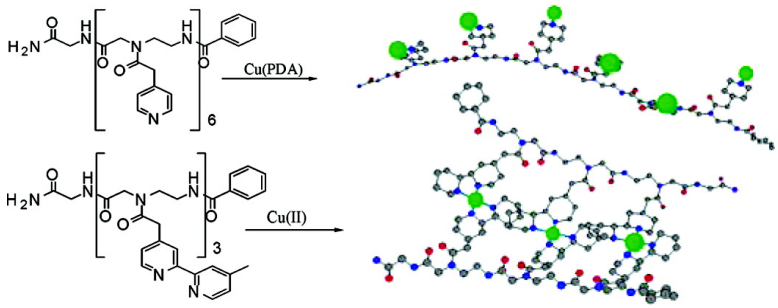

More About This Article

Additional resources and features associated with this article are available within the HTML version:

- Supporting Information
- Links to the 9 articles that cite this article, as of the time of this article download
- Access to high resolution figures
- Links to articles and content related to this article
- Copyright permission to reproduce figures and/or text from this article

View the Full Text HTML

J|A|C|S
ARTICLES
Published on Web 06/14/2005

Artificial Oligopeptide Scaffolds for Stoichiometric Metal Binding

Brian P. Gilmartin, Kristi Ohr, Rebekah L. McLaughlin, Richard Koerner, and Mary Elizabeth Williams*

Contribution from the Department of Chemistry, The Pennsylvania State University, 104 Chemistry Building, University Park, Pennsylvania 16802

Received February 19, 2005; E-mail: mbw@chem.psu.edu

Abstract: Two artificial peptides with pendant pyridine or bipyridine ligands have been synthesized and incorporated into oligomeric strands that are analogous to peptide nucleic acid. Spectrophotometric titrations with Cu^{2+} and Fe^{2+} show that the oligomers bind stoichiometric quantities of transition metals based on the number of pendant ligands. The identities of the titration products are confirmed by high resolution mass spectrometry. In the case of the bipyridine tripeptides, the titration stoichiometry and mass spectra indicate that the metal ions form interstrand cross-links between two oligopeptides, creating duplex structures linked exclusively by metal ions. Calculated molecular structures of the metalated oligopeptides and duplexes indicate that the peptide backbone acts as a scaffold for the directed assembly of metal ions. Electron paramagnetic resonance spectroscopy of the Cu-containing molecules have varying degrees of electronic interaction based on their charge and supramolecular structure. Cyclic voltammetry of the Fe^{2+}- and Cu^{2+}-linked bpy oligopeptide duplexes shows that they possess unique electrochemical signatures based on the redox reactivity of the metal complex.

Introduction

The molecular structure of deoxyribonucleic acid (DNA) contains the instructions for the production of genes and provides a uniquely elegant template for self-replication in biological systems. The double helical structure of DNA was first described by Watson and Crick in the middle part of the previous century, and it is well-known that the molecular recognition between individual strands making up this duplex results from hydrogen bonding between complementary base pairs that decorate the sugar phosphate backbone. Using DNA as a model, we synthesize artificial oligomeric peptides that are designed to exhibit the conformational structure of DNA but which self-assemble upon transition metal chelation. The metal binding base pairs should enhance the stability and binding affinity of duplex structures. In comparison with DNA, the wider range of transition metal complexes (metals and ligands) available for use in these structures greatly increases the number of possible complementary components.[1]

While nucleic acids (and in some cases the phosphate backbone) in DNA bind metal ions, their chelation affinities are relatively weak, leading to stoichiometries and geometries that are not well-defined or controllable. Construction of synthetic analogues allows the incorporation of distinct, high-affinity metal binding sites that circumvent these problems. To additionally avoid metal interaction with the sugar phosphates, we instead have chosen to utilize a peptidic backbone. The oligomer identified for our initial studies of the inorganic helicates is identical to that used for peptide nucleic acids (PNAs).[2] This peptide was chosen based on its (1) stability toward the enzymatic and chemical processes that can degrade the sugar−phosphate backbone of DNA and (2) easy adaptation toward large-scale automated synthesis. We utilize nitrogen-containing heterocyclic ligands with predictable binding affinities for transition metal ions to covalently link to the PNA peptide backbone in place of nucleic acids, as shown in Figure 1. These artificial peptide oligomers therefore serve as scaffolds

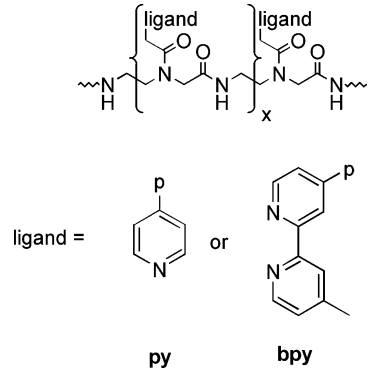

Figure 1. Structure of the polyamide backbone showing positions of attachments of *x* number of pendant ligrands. Below are the two ligands used in this study, where p indicates the point of attachment to the peptide backbone.

(1) (a) Henry, A. A.; Olsen, A. G.; Matsuda, S.; Yu, C.; Geíerstanger, B. H.; Romesberg, F. E. *J. Am. Chem. Soc.* **2004**, *126*, 6923−6931. (b) Ogawa, A. K.; Wu, Y.; McMinn, D. L.; Liu, J.; Schultz, P. G.; Romesberg, F. E. *J. Am. Chem. Soc.* **2000**, *122*, 3274−3287. (c) Neuner, P.; Monaci, P. *Bioconjugate Chem.* **2002**, *13*, 676−678.

(2) Nielsen, P. E.; Egholm, M.; Berg, R. H.; Buchardt, O. *Science* **1991**, *254*, 1497−1500.

10.1021/ja0510818 CCC: $30.25

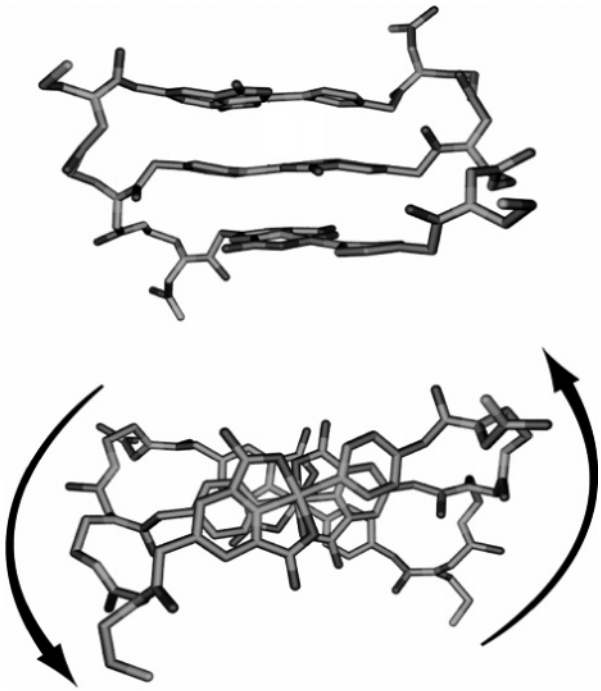

Figure 2. Side and top views of a calculated molecular model of a synthetic oligomeric helicate, formed by interstrand cross-linking of peptide strands by three metal ions.

for the stoichiometric binding of metals in a geometrically defined arrangement.

We predict that when metal ions are used to link these artificial peptides, a structure similar to those calculated and shown in Figure 2 will result. In these synthetic model systems, molecular recognition and interchain linking between the new "base pairs" is based entirely on a coordination chemistry motif rather than hydrogen bonding.[3,4] In addition to mimicking the helical *structure* of DNA, these multimetallic analogues mimic the information storage *function* of DNA, in that they are expected to exhibit unique optical and electronic properties that are strongly dependent on the peptide sequence and coordinated metals. The metal-decoroated peptides therefore provide the basis for new motifs of functional self-assembled nanostructures for possible use as inorganic "bar codes" and may provide opportunities for the development of biocompatible transition metal pharmacological agents.[5]

This paper presents the synthesis and characterization of oligopeptides bearing pyridine (py) and 2,2′-bipyridine (bpy) ligands, demonstrates the ability of these to bind stoichiometric quantities of transition metal ions to form multimetallic single and double stranded structures, and examines their electron paramagnetic resonance spectra and electrochemical properties.

Experimental Section

Chemicals. All materials were purchased from Aldrich and used as received unless otherwise noted. *N*,*N*-Diisopropylethylamine (DIPEA, Avocado) was distilled over CaH_2, and CH_2Cl_2 (VWR) was dried on an activated alumina column. For all experiments, ultrapure water was used (Labconco Water Pro PS system, 18.2 MΩ). Fmoc-aeg-OtBu·HCl,[6] aquo 2,2′:6′,2″-terpyridine copper(II) diperchlorate[7] (i.e., $[Cu(tpy)(H_2O)](ClO_4)_2$), and bis(aquo) pyridine-2,6-dicarboxyl copper(II)[8] (i.e., $[Cu(pda)(H_2O)_2]$) were prepared according to previously published procedures.

Oligomers were synthesized on an Fmoc-PAL-PEG-PS resin (Applied Biosystems). A 4-molar excess of the monomers and amino acids was used during coupling reactions; the targeted oligomer was synthesized on a 0.1 mmol scale, as determined by the maximum loading level of the resin.

Instrumentation and Analysis. High performance liquid chromatography (HPLC) was performed on a Varian system equipped with two quaternary pumps (model 210), an autosampler (model 410), UV−visible detector (model 320), and fraction collector (model 701). Preparatory scale separations were performed with a 100 × 20 mm^2 C_{18} column (S-5 μm, 12 nm, YMC, Co.) and a 2 mL injection loop. Elution of the product was detected using the pyridine absorbance at 255 nm.

Positive ion electrospray ionization (ESI+) mass spectrometry was performed on a Mariner mass spectrometer (PerSeptive Biosystems). Theoretical mass spectrometry peaks and relative intensities were calculated using software available at http://www2.sisweb.com/mstools/isotope.htm.

Electrochemical data were collected with a CH Instruments model 660A potentiostat with a picoamp booster. Solutions were prepared from doubly distilled acetonitrile and thoroughly deoxygenated. Voltammetry was obtained using a 12.5 micron radius Pt working electrode, 2 mm diameter Pt wire counter electrode, and 22 gauge Ag wire quasi-reference electrode. The obtained voltammograms were manually corrected for uncompensated resistance.

Circular dichroism (CD) spectroscopy was performed using a Jasco J-810 spectropolarimeter with a quartz cell with an optical path length of 1 mm. Experiments were performed at room temperature with a bandwidth of 1 nm and wavelength increment of 1 nm.

All NMR spectra were obtained with either a Bruker 300 or 400 MHz spectrometer at room temperature. X-band EPR spectra were obtained using a 9.5 GHz Bruker eleXsys 500 spectrometer equipped with a liquid helium cryostat. All experiments were performed at 16 K, with a modulation frequency of 100 kHz and modulation amplitude of 5 G. For $[Cu(\mathbf{2})_2]_3(PF_6)_6$ and $[Cu(pda)(\mathbf{1})]_6$, the microwave power was 8.23 mW; for $[Cu(tpy)(\mathbf{1})]_6(ClO_4)_{12}$, it was 0.15 mW.

Molecular structures were calculated using Hyperchem 6.0 using molecular mechanics (MM+) with atomic charge based electrostatic repulsions and a Polack-Ribiere conjugate gradient to a minimum energy gradient of 0.01 kcal/mol.

Synthesis. A. Fmoc-aeg(py)-OH·HCl (1): A mixture of 4.057 g (0.010 23 mol) of Fmoc-aeg-OtBu·HCl, 2.374 g of 1-[(3-dimethylamino)-propyl]-3-ethylcarbodiimide (EDC, 0.012 38 mol), 2.200 g (0.012 67 mol) of 4-pyridylacetic acid hydrochloride, 6.50 mL (0.0373 mol) of

(3) (a) Zelder, F. H.; Mokhir, A. A.; Krämer, R. *Inorg. Chem.* **2003**, *42*, 8618−8620. (b) Mokhir, A.; Stiebing, R.; Kraemer, R. *Bioorg. Med. Chem.* **2003**, *13*, 1399−1401. (c) Verheijen, J. C.; van der Marel, G. A.; van Boom, J. H.; Metzler-Nolte, N. *Bioconjugate Chem.* **2000**, *11*, 741−743.

(4) (a) Popescu, D.-L.; Parolin, T. J.; Achim, C. *J. Am. Chem. Soc.* **2003**, *125*, 6354−6355. (b) Atwell, S.; Meggers, E.; Spraggon, G.; Schultz, P. *J. Am. Chem. Soc.* **2001**, *123*, 12364−12367. (c) Meggers, E.; Holland, P. L.; Tolman, W. B.; Romesberg, F. E.; Schultz, P. *J. Am. Chem. Soc.* **2000**, *122*, 10714−10715. (d) Tanaka, K.; Tengiji, A.; Kato, T.; Toyama, N.; Shionoya, M. *Science* **2003**, *299*, 1212−1213. (e) Tanaka, K.; Shionoya, M. *J. Org. Chem.* **1999**, *64*, 5002−5003. (f) Weizman, H.; Tor, Y. *J. Am. Chem. Soc.* **2001**, *123*, 3375−3376. (g) Weizman, H.; Tor, Y. *Chem. Commun.* **2001**, *5*, 453−454.

(5) (a) Blower, P. J.; Dilworth, J. R.; Mullen, R. I.; Reynolds, C. A.; Zheng, Y. *J. Inorg. Biochem.* **2001**, *85*, 15−22. (b) Kurosaki, H.; Sharma, R. K.; Aoki, S.; Inoue, T.; Okamoto, Y.; Sugiura, Y.; Doi, M.; Ishida, T.; Otsuka, M.; Goto, M. *J. Chem. Soc., Dalton Trans.* **2001**, 441−447. (c) Lebon, F.; Boggetto, N.; Ledecq, M.; Durant, F.; Benatallah, Z.; Sicsic, S.; Lapouyade, R.; Kahn, O.; Mouithys-Mickalad, A.; Deby-Dupont, G.; Reboud-Ravaux, M. *Biochem. Pharm.* **2002**, *63*, 1863−1873.

(6) Thomson, S. A.; Josey, J. A.; Cadilla, R.; Gaul, M. D.; Hassman, C. F.; Luzzio, M. J.; Pipe, A. J.; Reed, K. L.; Ricca, D. J.; Wiethe, R. W.; Noble, S. A. *Tetrahedron* **1995**, *51*, 6179−6194.

(7) Ohr, K. The Pennsylvania State University, unpublished results.

(8) (a) Murtha, D. P.; Walton, R. A. *Inorg. Chim. Acta* **1974**, *8*, 279−284. (b) Ullah, M. R.; Bhattacharya, P. K. *Indian J. Chem., Sect. A* **1991**, 976−978.

DIPEA, and 300 mL of CH_2Cl_2 was stirred for 1 h under N_2. The yellow solution was extracted with H_2O (5 × 100 mL). The combined aqueous washings were extracted with CH_2Cl_2 (50 mL). The combined organic extracts were dried over anhydrous Na_2SO_4 and flash evaporated to give a yellow oil. The oil was stirred in an aqueous solution of 3 M HCl (150 mL). The acid was removed under reduced pressure to yield a yellow oil, which was dried for 16 h under vacuum. The pure product was obtained by recrystallization from CH_3CN, followed by vacuum-drying for 16 h. Yield = 2.235 g (48.1%) (^{1}H NMR, 300 MHz, d_6-DMSO): 3.08 (m, 1 H); 3.18 (m, 2 H); 3.29 (m, 2 H); 3.40 (m, 2 H); 3.91 (d, 2 H); 4.05 (s, 1 H); 4.13 (m, 1 H); 4.22 (m, 3 H); 7.23 (t, 2 H); 7.31 (t, 2 H); 7.41 (t, 1 H); 7.59 (d, 2 H); 7.72 (t, 2 H); 8.80 (d, 2 H); 8.71 (d, 2 H).

B. Fmoc-aeg(bpy)-OH·HCl (2): Fmoc-aeg-O*t*Bu·HCl (1.333 g, 0.003 08 mol) was dissolved in $CHCl_3$ (100 mL) and washed with an aqueous solution of saturated $NaHCO_3$ (3 × 100 mL). The washings were extracted with $CHCl_3$ (50 mL). The organics were then dried over Na_2SO_4, and the solvent was removed under vacuum leaving a clear oil. A solution of 4′-methyl-2,2′-bipyridine-4-acetic acid[9] (1.004 g, 0.004 40 mol), 2-(1*H*-benzotriazole-1-yl)-1,1,3,3-tetramethyluronium hexafluorophosphate (HBTU, Novabiochem, 2.236 g, 0.005 90 mol), and DIPEA (1.015 mL, 0.005 84 mol) in *N*,*N*-dimethylformamide (DMF, 100 mL) was prepared, added to the oil, and was stirred under N_2 for 2 h. The *tert*-butyl-protected product was then precipitated by addition of the solution to ice water (1.3 L). The precipitate was collected by filtration and dried in vacuo overnight, leaving a yellow solid. The solid was dissolved in a solution of 2.5% water in trifluoroacetic acid (TFA, 10 mL). The solution was stirred for 2 h and then precipitated from cold ethyl ether (Et_2O, 200 mL), giving the product as an off-white powder. Yield = 1.014 g (49.6%) (^{1}H NMR, 300 MHz, d_6-DMSO): 2.50 (s, 3 H); 3.17 (t, 1 H); 3.28 (t, 1 H); 3.38 (t, 1 H); 3.49 (t, 1 H); 3.84 (s, 1 H); 4.00 (d, 2 H); 4.25 (m, 4 H); 7.29 (t, 2 H); 7.40 (t, 2 H); 7.53 (m, 2 H); 7.65 (t, 2 H); 7.87 (d, 2 H); 8.37 (s, 2 H); 8.65 (m, 2 H). (ESI+) Calculated: $(m + H)^+ = 551.2$. Found: $(m + H)^+ = 551.3$.

C. R_1-(1)$_6$$R_2$-NH$_2$ (R_1 = Acetyl (Ac) or Benzyl (Bz); R_2 = Lysine (K) or Glycine (G)). The oligomer was synthesized at room temperature on a Pioneer peptide synthesis system (Applied Biosystems) with DMF as the solvent. A solution of 20% piperidine in DMF (Applied Biosystems) was used for Fmoc-deprotection (5 min), and 0.5 M diisopropylcarbodiimide (DIPCDI, Applied Biosystems) and 0.5 M DIPEA were used for the couplings (30 min). A capping cycle was performed after every coupling with 0.5 M benzoic anhydride (Avocado) or 0.5 M acetic anhydride and 0.5 M DIPEA (5 min).

Following synthesis, the resin was washed 3 × 10 mL with DMF, followed by 3 × 10 mL alternating 2-propanol and CH_2Cl_2. The oligomer was cleaved from the resin by stirring the resin with 10 mL of 2.5% H_2O, 2.5% triisopropylsilane (TIS) in TFA for 2 h. The mixture was filtered in 4 equal volumes through a glass frit into 4 × 40 mL of cold Et_2O. The solutions were mixed and kept at 0 °C for 1 h. The oligomer was collected by centrifugation as pale yellow pellets and washed 3 × 10 mL with Et_2O and dried under vacuum for 1 h.

Purification of the oligomer (the major product) was accomplished by preparatory scale HPLC using a gradient elution of 5% (0.1% TFA in CH_3CN):95% (0.1% TFA in H_2O) to 15% (0.1% TFA in CH_3CN): 85% (0.1% TFA in H_2O) ramped over 13 min with a total flow of 20 mL/min and a fraction collection program. TFA and CH_3CN were removed from the collected fractions under reduced pressure, and H_2O was removed by lyophilization. Overall [Bz-(**1**)$_6$G-NH$_2$] yield = 0.072 g (33%) (^{1}H NMR, 300 MHz, d_6-DMSO): 3.15−3.75 (m, 26 H); 3.75−4.30 (m, 24 H); 7.08 (s, 1 H); 7.21 (s, 1 H); 7.50 (m, 4 H); 7.71 (m, 14 H); 8.01 (m, 1 H); 8.30 (m, 3 H); 8.50 (m, 2 H); 8.70 (m, 12 H). Further confirmation of purity and identity were accomplished with COSY, HMQC, and HMBC NMR; see Supporting Information. (ESI+) Calculated: $(m + H)^+ = 1493.7$, $(m + Na)^+ = 1515.6$. Found: $(m + H)^+ = 1493.8$, $(m + Na)^+ = 1515.7$.

D. Bz-(2)$_3$G-NH$_2$. A 25 mL fritted polypropylene reservoir (Alltech) was used in the synthesis of the oligomer. The reservoir was heated to ∼50 °C with electric heating tape (Barnstead/Thermolyne), and N_2 was bubbled through the DMF solution. The synthesis uses 20% piperidine in DMF for Fmoc-deprotection (15 min), and solutions of 0.5 M HBTU and 0.5 M DIPEA for monomer and amino acid coupling (30 min), and 0.5 M benzoic anhydride and 0.5 M DIPEA in DMF for capping (5 min). Each coupling step was monitored for completion using a Kaiser test.[10] After the desired number of cycles, the resin was washed 3 × 10 mL with DMF, followed by 3 × 10 mL CH_2Cl_2. The oligomer was cleaved from the resin by stirring the resin with 10 mL of 2.5% H_2O, 2.5% TIS in TFA for 2 h. The mixture was filtered in 4 equal volumes through a glass frit into 4 × 40 mL of cold Et_2O. The oligomer was collected as pale yellow pellets by centrifugation, and the pellets washed with 3 × 30 mL with Et_2O and dried under vacuum for 1 h.

The desired oligomer was separated from deletion sequences using an HPLC gradient elution of 10% (0.1% TFA in CH_3CN):90% (0.1% TFA in H_2O) ramped to 28% (0.1% TFA in CH_3CN):72% (0.1% TFA in H_2O) over 15 min at 20 mL/min. After fraction collection, the oligomer was lyophilized to give a pale pink solid. Overall Bz-(**2**)$_3$G-NH$_2$ yield = 1.2 mg (1.19%). (^{1}H NMR, 400 MHz, MeOH-d_4): 2.22−2.41 (m, 9 H); 3.38−4.32 (m, 26 H); 7.00−8.59 (m, 23 H). Identification of these peaks and confirmation of purity were accomplished with HMQC NMR; see Supporting Information for detailed analysis. (ESI+) Calculated: $(m + H)^+ = 1109.5$. Found: $(m + H)^+ = 1109.4$, $(m + Na)^+ = 1131.5$, $(m + K)^+ = 1147.5$.

Spectrophotometric Titrations. A. Bz-(1)$_6$G-NH$_2$ + [Cu(pda)(H$_2$O)$_2$] or [Cu(tpy)(H$_2$O)$_2$](ClO$_4$)$_2$. Titrations were performed using a Varian Cary 500 spectrophotometer. A solution of the Bz-(**1**)$_6$G-NH$_2$ was prepared in methanol (MeOH). The concentration of the oligomer (2.222 mM) was determined using its molar extinction coefficient (ϵ = 31 860 M^{-1} cm^{-1}) at 256 nm. This solution was titrated in 5, 10, and 20 μL increments into 2.5 mL of a 0.6608 mM [Cu(pda)(H_2O)$_2$] methanolic solution at 4 min intervals between each addition. For each addition, the reference solution was diluted with an equal volume of MeOH to account for concentration effects. UV−visible absorption spectra were acquired for each iterative addition of oligomer. The titration product was precipitated by slow addition of ether, filtered, rinsed with ether, and reprecipitated from methanol. Titrations with [Cu(tpy)(H_2O)](ClO$_4$)$_2$ were performed analogously using a 2.804 mM methanolic solution containing a small amount (3.361 μM) H_2O. The titration product was isolated as for the [Cu(pda)] adduct.

B. Fe(ClO$_4$)$_2$ + Bz-(2)$_3$G-NH$_2$. Titrations were performed on a Varian Cary 50 spectrophotometer. A solution of Bz-(**2**)$_3$G-NH$_2$ was prepared, and the concentration was determined to be 70.8 μM using its molar extinction coefficient (ϵ = 6322.6 M^{-1} cm^{-1}) at 284 nm. A solution of 784 μM [Fe(ClO$_4$)$_2$] in MeOH was added in 2 μL increments to the oligomer solution in 5 min intervals, and UV−visible absorption spectra were obtained for each addition. The titration products were precipitated with NH_4PF_6, the supernatant was decanted, and the solid was rinsed with copious amounts of water.

C. Cu(OAc)$_2$ + Bz-(2)$_3$G-NH$_2$. This titration was performed similarly to that from the Fe(ClO$_4$)$_2$ experiment, except that a 734.5 μM Bz-(**2**)$_3$G-NH$_2$ solution in MeOH was titrated with a solution of 9.29 mM Cu(OAc)$_2$ in MeOH in 20 μL increments at 15 min intervals. Spectra were corrected for the background absorbance of unbound Cu acetate. The titration product was isolated and purified as above. Elemental Analysis Calculated: 47.99%, C; 4.64%, H; 11.87%, N. Found: 47.72%, C; 4.96%, H; 12.04%, N.[11]

(9) Della Ciana, L.; Hamachi, I.; Meyer, T. J. *J. Org. Chem.* **1989**, *54*, 1731−1735.

(10) Kaiser, E.; Colescott R. L.; Bossinger, C. D.; Cook, P. I. *Anal. Biochem.* **1970**, *34*, 595−598

(11) Insufficient quantities of material were available to quantitatively determine the percentage of metal ion in the sample.

Scheme 1. Synthesis of Ligand−Peptide Monomers and Structures of the Oligomers; Ac = Acetyl; Bz = Benzoyl; G = Glycine; K = Lysine

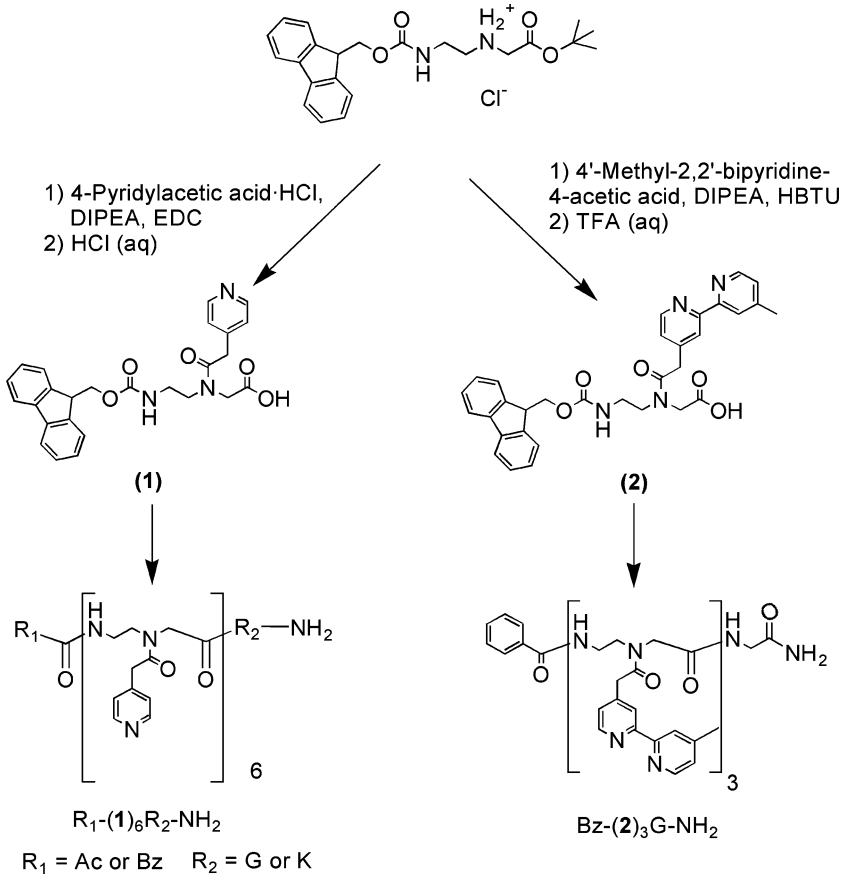

Results and Discussion

Synthesis. Py and bpy were chosen as the initial target ligands for incorporation onto the peptide backbone because of their wide use in coordination chemistry for a variety of transition metals. To prepare peptides incorporating these pendant ligands, we use standard solid-phase synthesis methods. The peptide/ligand monomers were prepared according to the method shown in Scheme 1 from their acetic acid derivatives,[12,13] by adaptation of a literature procedure.[6] Briefly, the ligands were reacted with Fmoc-protected *N*-[2-aminoethyl] glycine *tert*-butyl ester (Fmoc-aeg-O*t*Bu·HCl) using *N*,*N*-diisopropylethylamine (DIPEA) and the coupling reagent shown in Scheme 1. Amide coupling to the py ligand was accomplished with DIPEA and EDC at 25 °C for 1 h. The bpy analogue required the use of DIPEA and HBTU. For both ligands, the terminal acid was deprotected by acid cleavage of the *tert*-butyl to yield monomers **1** and **2** with overall yields 48% and 50%, respectively.

Oligomers were prepared from monomers **1** and **2** by solid-phase synthetic methods[6] on a resin support (Fmoc-PAL-PEG-PS, Applied Biosystems). Oligomers were typically prepared using an automated peptide synthesizer (Applied Biosystems Pioneer System), which enables the facile preparation of sequences of varying length and composition.[7] In some cases, resin-supported synthesis was performed by hand. For the py hexamer, we prepared both the lysine- and glycine-linked oligomers and the benzoyl- and acetyl-terminated chains, as indicated in Scheme 1. These slight modifications in the peptide backbone have no substantial effects on the physical properties of the py oligomers. For the sake of clarity, we detail the synthesis and metal binding of the two oligomer sequences shown in Scheme 1, a py hexamer, Bz-(**1**)$_6$G-NH$_2$, and bpy trimer, Bz-(**2**)$_3$G-NH$_2$.

The oligomers were cleaved from the resin using an excess quantity of 2.5% water and 2.5% triisopropylsilane (TIS) in trifluoroacetic acid (TFA), giving the oligomers shown in Scheme 1. The products were separated from deletion sequences and reaction byproducts by reverse-phase high-performance liquid chromatography (HPLC), and the desired fraction was collected and lyophilized to yield the purified oligomer. For Bz-(**1**)$_6$G-NH$_2$, the final yield of the hexamer was 33% (based on the loading of the resin) and purity was confirmed by NMR and mass spectrometry. The typical yield of the Bz-(**2**)$_3$G-NH$_2$ was 1.19%, with purity again confirmed by NMR and mass spectrometry. Detailed analysis of the two-dimensional NMR spectra (COSY and HMQC), which confirms the purity of the oligopeptides, is found in the Supporting Information. The significantly lower yield of the bpy oligomer is thought to arise from both steric hindrance and aggregation induced by π-stacking of the ligands, and our ongoing efforts seek to improve the overall yield for this and other multidentate ligand oligomers.[14]

Metal Coordination to Pyridine Hexamer. We next investigated the ability of the artificial peptide oligomers to bind transition metal ions. Since it is well-known that metal

(12) Sasse, W. H. F.; Whittle, C. P. *J. Chem. Soc.* **1961**, *83*, 1347−1350.
(13) Kim, B. H.; Lee, D. N.; Park, H. J.; Min, J. H.; Jun, Y. M.; Park, S. J.; Lee, W.-Y. *Talanta* **2004**, *62*, 595−602.
(14) Gilmartin, B. P.; Pantzar, L. The Pennsylvania State University, unpublished results.

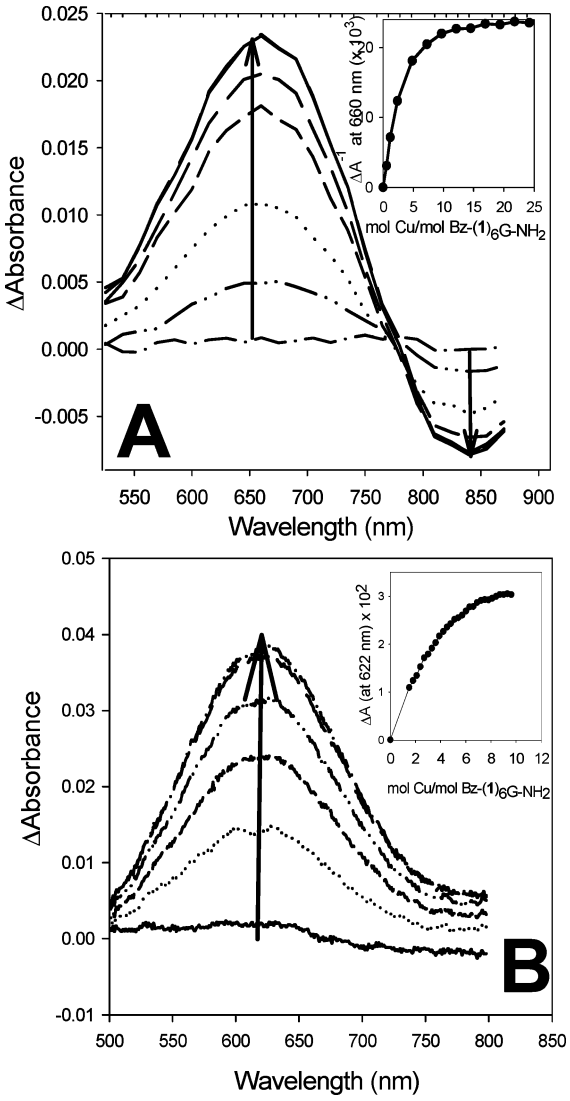

Figure 3. UV−visible absorption spectroscopy difference spectra for the titration of Bz-(**1**)$_6$G-NH$_2$ with (A) [Cu(pda)] and (B) [Cu(tpy)]$^{2+}$. The insets contain plots of the peak absorbance as a function of relative molar ratio of metal ion to oligomer.

coordination is typically accompanied by the appearance of a peak in the UV−visible absorption spectrum, we used spectrophotometric titrations to monitor the complexation of Cu^{2+} and Fe^{2+} ions to the oligomers. We chose to strictly enforce one-to-one complexation to the pyridine hexamers (i.e., one metal to each pendant ligand) to confirm the availability of each of the ligands for chelation. Therefore, tetracoordinate metal ions bearing tridentate ligands (i.e., [Cu(pda)] and [Cu(tpy)]$^{2+}$) were used to preferentially bind to the pendant pyridine oligomers to fill their coordination shell.[8] Figure 3A shows the difference spectra for the change in visible absorbance resulting from the titration of a methanolic solution of Bz-(**1**)$_6$G-NH$_2$ oligomer with [Cu(pda)(H$_2$O)$_2$].[8] The peak at 660 nm, associated with a [Cu(pda)(py)] absorption, increases during early additions of oligomer and reaches a maximum value. A negative change in absorbance at 840 nm is simultaneously observed and is attributed to the consumption of free [Cu(pda)] in solution. The titration curve for this experiment, plotted as the change in absorbance as a function of added oligomer, is shown in the Figure 3A inset. This curve indicates that the growth of the [Cu(pda)(py)] absorption peak begins to level at a maximum value of ~6 molar equivalents of [Cu(pda)] per mole of Bz-(**1**)$_6$G-NH$_2$.[15] Metal complexation of the acetyl capped, lysine analogue (i.e., Ac-(**1**)$_6$K-NH$_2$) has the same metal binding stoichiometry (not shown; see mass spectrometry data in the Supporting Information). These spectrophotometric data strongly suggest the formation of an oligomeric strand of Bz-(**1**)$_6$G-NH$_2$ with six bound [Cu(pda)] centers, (Bz-[Cu(pda)(**1**)]$_6$G-NH$_2$).

High-resolution ESI+ mass spectrometry was employed to analyze the purified titration product; the observed molecular ion peak at 1460.7 m/z ($z = +2$, (m + 2Na$^+$)) agrees well with the calculated mass of 2869.4 amu (i.e., an expected (m + 2Na$^+$) $z = +2$ peak at 1459.7 m/z), confirming the py hexamer with a stoichiometric quantity of bound [Cu(pda)] is the titration product (Bz-[Cu(pda)(**1**)]$_6$G-NH$_2$).

To test the effect of ionic charge on the addition of complexes to the pyridine oligomers, Bz-(**1**)$_6$G-NH$_2$ was also titrated with [Cu(tpy)](ClO$_4$)$_2$. Figure 3B shows the difference spectra collected during the titration of Bz-(**1**)$_6$G-NH$_2$ with [Cu(tpy)]$^{2+}$, together with the titration curve (Figure 3B, Inset) that conclusively demonstrates the formation of the complex (Bz-[Cu(tpy)(**1**)]$_6$-G-NH$_2$)(ClO$_4$)$_{12}$. The Cu complexes in (Bz-[Cu(tpy)(**1**)]$_6$-G-NH$_2$) each have a +2 charge, so that the overall charge of the metal-coordinated oligopeptide is +12, versus the charge-neutral (Bz-[Cu(pda)(**1**)]$_6$-G-NH$_2$) species. Importantly, stoichiometric complexation is observed despite the large positive charge, indicating that electrostatic repulsion between metal centers is unimportant for binding. The isolated solid products of these multimetallic structures are finely divided powders, and our attempts to grow crystallographic quality crystals have been fruitless to date. However, we have used molecular modeling to predict and understand these molecules, discussed further below.

Metal Coordination by Bpy Oligmer. The bpy ligand in Bz-(**2**)$_3$G-NH$_2$ is bidentate toward transition metals and therefore provides a distinctly different binding motif than the (monodentate) py oligopeptide. Because of the presence of tridentate ligands coordinated to the tetracoordinate metal center, the [Cu(pda)] and [Cu(tpy)]$^{2+}$ complexes used in the titrations of the py oligomer do not bind to the bidentate bpy ligands and were therefore not used to study binding to the bpy tripeptide. However, it is known that free Fe^{2+} ions form hexacoordinate complexes with bpy (i.e., [Fe(bpy)$_3$]$^{2+}$), whereas Cu^{2+} ions form the tetracoordinate complex [Cu(bpy)$_2$]$^{2+}$. In the absence of other ligands, metal ions added to solutions containing Bz-(**2**)$_3$G-NH$_2$ should coordinate to multiple bpy ligands to form inter- and/or intrachain linkages. Metal complexation could also induce the formation of undesired coordination polymers, which we prevent by use of solutions with low oligomer and metal concentration.[16] Spectrophotometric titrations of dilute solutions of the Bz-(**2**)$_3$G-NH$_2$ oligomer were performed with Fe^{2+} perchlorate (Fe(ClO$_4$)$_2$) and Cu^{2+} acetate (i.e., Cu(OAc)$_2$). Figure 4A shows the change in visible absorbance during the addition of Fe(ClO$_4$)$_2$ to a methanolic solution of Bz-(**2**)$_3$G-NH$_2$; the strong peak at 540 nm is the well-known metal-to-

(15) The slight rise in absorbance beyond the equivalence point is likely a result of either background absorbance of free [Cu(pda)] in solution, whose broad absorbance peak overlaps the [Cu(pda)(py)] transition, or the slow chelation kinetics.

(16) No polymerization products have been observed under dilute solution conditions; however these are expected to be large and insoluble, and the reaction solutions are filtered prior to precipitation of the desired material.

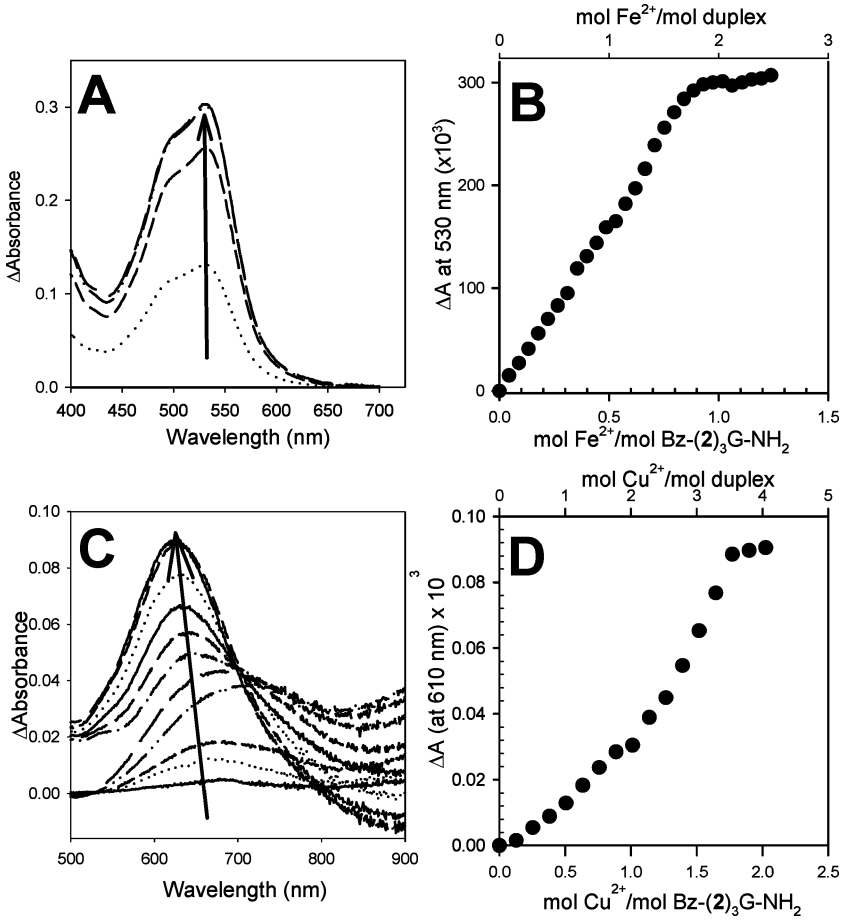

Figure 4. UV−visible absorption spectroscopy difference spectra for the titration of Bz-(**2**)$_3$G-NH$_2$ with (A) Fe(ClO$_4$)$_2$ and (C) Cu(OAc)$_2$. (B and D) Plots of the peak absorbance as a function of relative molar ratio of metal ion to oligomer for the Fe^{2+} and Cu^{2+} ions, respectively.

ligand charge transfer (MLCT) transition for $[Fe(bpy)_3]^{2+}$.[17] The titration curve in Figure 4B shows that the intensity of the MLCT peak increases upon addition of Fe^{2+} and levels off at a stoichiometric equivalence point of 1 mol of Fe^{2+}:1 mol of Bz-(**2**)$_3$G-NH$_2$.

Two possible structures would be consistent with this stoichiometric ratio: either one oligopeptide coordinated to a single Fe^{2+} ion, [Bz-[Fe(**2**)$_3$]G-NH$_2$)$_2$] (i.e., [Fe(**2**)$_3$], calculated mass 1164.4 amu), or two oligopeptides cross-linked by two Fe^{2+} ions to form [Bz-[Fe(**2**)$_3$]G-NH$_2$)]$_2$ (i.e., [Fe(**2**)$_3$]$_2$, calculated mass 2328.8 amu). High-resolution mass spectrometry was used to identify which of these was the titration product, and a molecular ion was observed at 583.7 *m*/*z*. Both the $z = +2$ ion of [Fe(**2**)$_3$] and the $z = +4$ ion of [Fe(**2**)$_3$]$_2$ are expected to have peaks at this *m*/*z* ratio. However, analysis of the observed isotopic splitting of the high-resolution molecular ion peak evidences sharp peaks with 0.25 *m*/*z* separation, consistent with an ion of $z = +4$ charge. Therefore, the high-resolution mass spectrometry data leads to the conclusion that the titration product is an *oligopeptide duplex linked by two bound* Fe^{2+} *ions.*[18]

To unambiguously confirm that metal coordination can be utilized to induce duplex formation, we also titrated the Bz-(**2**)$_3$G-NH$_2$ oligomer with [Cu(OAc)$_2$],[19] which we reasoned would have a different stoichiometric equivalence point based on the tetracoordinate nature of Cu^{2+}. Visible absorption spectra were again collected during the titration, Figure 4C. These spectra contain a peak at 610 nm that grew and reached a maximum value in the titration curve in Figure 4D at a Cu^{2+}/oligomer equivalence point of ∼1.6. This molar ratio is consistent with either a single bpy tripeptide binding 1.5 Cu^{2+} ions to form [Bz-[Cu(**2**)$_2$]$_{1.5}$G-NH$_2$]$_2$ (i.e., [Cu(**2**)$_2$]$_{1.5}$, calculated mass 613.0 amu) or two bpy tripeptides linked by three Cu^{2+} ions to make [Bz-[Cu(**2**)$_2$]$_3$G-NH$_2$]$_2$ (i.e., [Cu(**2**)$_3$]$_2$, calculated mass 1225.9 amu). Elemental analysis of the titration product, isolated in larger quantity (∼3 mg) than the Fe analogue (<1 mg), confirmed its purity but could not differentiate between the two possible structures. However, analysis of the product using high-resolution mass spectrometry revealed a $z = +2$ molecular ion peak (based on the isotopic splitting) at 1227.7 *m*/*z*. This molecular ion peak is consistent with the calculated molecular weight of the [Cu(**2**)$_3$]$_2$ *duplex* structure, and taken together, these data strongly suggest the formation of an *oligopeptide duplex linked by three* Cu^{2+} *ions.*

In both the Fe and Cu bpy oligopeptide duplex cases, the isolated metal-containing molecules form finely divided powders, which likely results from the large number of possible structural isomers. Figure 5 shows just two examples (for each

(17) Lever, A. B. P. *Inorganic Electronic Spectroscopy*; Elsevier Publishing Co.: New York, 1968.
(18) Because of the very small quantities of this duplex that were produced, elemental analysis of this titration product was not possible.
(19) Cu^{2+} ion complexation is kinetically slower than Fe^{2+} binding, requiring longer equilibration times between iterative additions. The difference spectra show free Cu acetate ions (λ > 650 nm) because of a lower equilibrium binding constant.

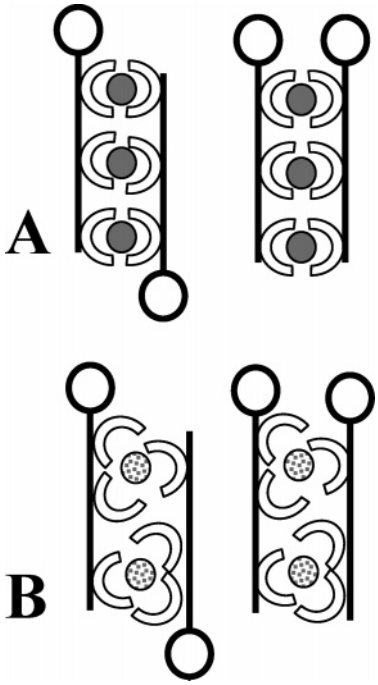

Figure 5. Schematic diagrams of bipyridine tripeptides linked by (A) three tetracoordinate (e.g., Cu^{2+}) ions and (B) two octahedral (e.g., Fe^{2+}) ions. Circles on chain termini indicate benzoyl or acetyl caps.

of the metals) of the possible isomers that result from antiparallel vs parallel alignment of the oligopeptides, an asymmetry that arises from the sequence of the chain and the different termini. *Many* more structures are possible based on changes in the metal−ligand connectivity and the asymmetry of the bipyridine, which is attached only in the 4-position.[20] Coupled together, the structural isomers and the small quantity of prepared metalated material have made crystallization of the metal-linked duplexes impossible to date. Our continuing efforts are focused on the preparation of large enough quantities of the oligopeptides to enable the isolation of a single isomer.

Molecular Modeling. To better understand the molecular structures of the metal-coordinated pyridine hexapeptides and the metal-linked bpy tripeptide duplexes, we have turned to computational molecular modeling. In the cases of the former oligopeptides, because the metal complexes decorate a single peptide chain, we expected a large amount of disorder in the calculated structures. Figure 6A contains the energy minimized structure of $[Cu(pda)(\mathbf{1})]_6$, shown without the terminal benzoyl and glycine caps for clarity, from the side and top. In agreement with the crystal structures that we have obtained for the small molecule analogue [Cu(pda)(py)], the bound Cu complexes each have a square planar geometry. The most striking feature of this calculated structure is the twist of the oligopeptide backbone around the column of Cu metal complexes, most likely a result of $\pi-\pi$ interactions of the pda ligands, with a helical pitch of 16−17 monomers. The oligopeptide strand constrains the Cu centers to a columnar arrangements with a regular spacing of ~4 Å.

In contrast, molecular modeling of the $[Cu(tpy)(\mathbf{1})]_6^{+12}$ molecule is shown in Figure 6B. The metal complexes are splayed apart with an average distance of 20 Å. We justify the

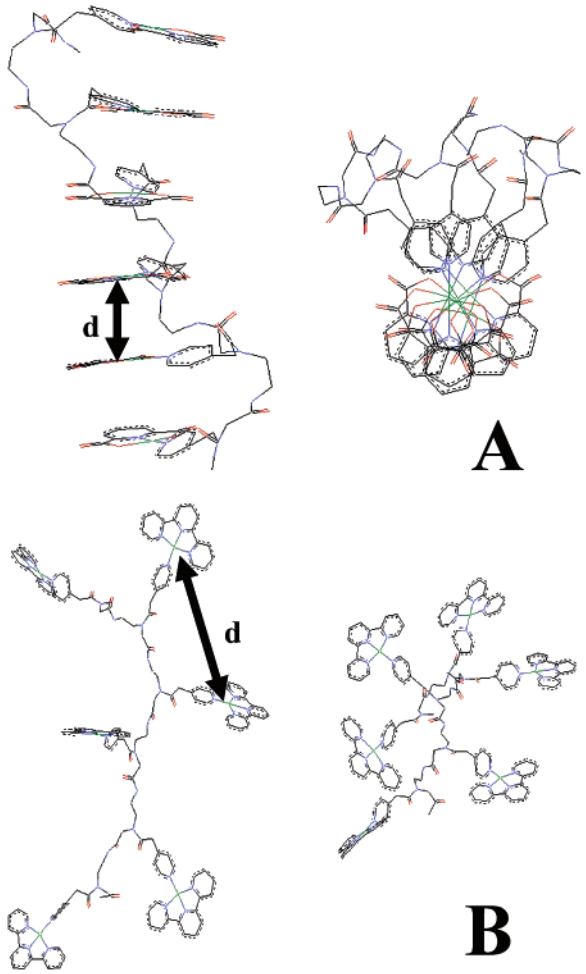

Figure 6. Energy-minimized structures of (A) $[Cu(pda)(\mathbf{1})]_6$ and (B) $[Cu(tpy)(\mathbf{1})]_6^{+12}$ calculated using MM+ (Hyperchem 6.0) from (left) side view and (right) top. Cu−Cu distances are (A) $d = 4.4$ Å and (B) average ~20 Å. Hydrogen atoms and oligomer termini are omitted for clarity.

differences between the calculated structures in Figure 6A and B based on the charge of the Cu complexes, where electrostatic repulsions between the $[Cu(tpy)(\mathbf{1})]^{2+}$ complexes prevents π stacking of the aromatic ligands. The structures in Figure 6 predict that, in the solid form, the degree of electronic interaction between Cu centers is much larger in the charge-neutral $[Cu(pda)(\mathbf{1})]_6$ structure than in the $[Cu(tpy)(\mathbf{1})]_6^{12+}$ complex. These differences are not expected to exist in solutions of these multimetallic molecules.

We also performed calculations on the metal-linked bpy tripeptide duplexes to visualize the most stable possible isomers. Figure 7 contains the energy minimized, calculated structures (shown from the side and top) for the $[Cu(\mathbf{2})_2]_3$ and $[Fe(\mathbf{2})_3]_2$ duplexes. In each of these calculated structures, the oligopeptide acts as a scaffold to hold the metal complexes in close proximity: for the Cu^{2+} and Fe^{2+} duplexes, the metal centers are separated by 4.8 and 11 Å, respectively. In comparison with the molecular structures in Figure 6, the spacing between the Cu atoms in the duplex shown in Figure 7 is similar to that predicted for $[Cu(pda)(\mathbf{1})]_6$. It is evident from the models that differing metal coordination geometries dramatically affect the orientation of the peptide chains: whereas the octahedral Fe^{2+} complexes twist the peptide into a knotlike structure, the (distorted) square planar geometry of the Cu^{2+} complexes allows

(20) Ignoring possible rotamers of the bpy ligand around the ligand−peptide bond, which gives hundreds of geometric isomers, there are 12 possible tri-copper and 14 possible di-iron duplexes.

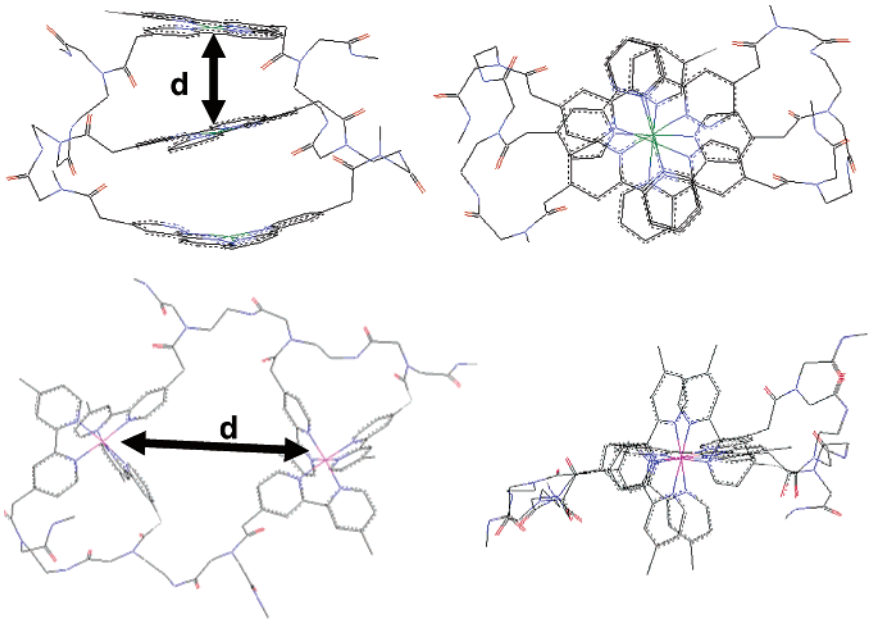

Figure 7. Energy-minimized structures of (A) $[Cu(\mathbf{2})_2]_3$ and (B) $[Fe(\mathbf{2})_3]_2$ duplexes, calculated using MM+ (Hyperchem 6.0), from the side and top. Calculated Cu−Cu distances are $d = 4.8$ Å; Fe−Fe distance is $d = 11$ Å. Hydrogen atoms and oligomer termini are omitted for clarity.

the peptide strands to adopt a helical confirmation with a pitch of ∼18 monomers.

Electron Paramagnetic Resonance Spectroscopy. Since electron paramagnetic resonance (EPR) spectroscopy is sensitive to the local environment and coupling between paramagnetic species, we next turned to analysis of the metalated oligopeptides to provide additional insight into their structures. Frozen EPR spectra were obtained in methanolic solutions at 16 K for each of the oligopeptides with bound Cu (ions or complexes) and are shown in Figure 8. Values of the EPR spectroscopy parameters and coupling constants are given in Table 1. The spectrum for the pyridine hexapeptide with six-coordinated $[Cu(tpy)]^{2+}$ complexes (i.e., $[Cu(tpy)(\mathbf{1})]_6^{12+}$) (Figure 8A) has the classic line shape for a Cu complex with a hyperfine coupling of $A_{||} = 167 \times 10^{-4}$ cm^{-1}.[21] While this spectrum would be expected for a single Cu complex, this observation for the hexametallic peptide implies that each of the $[Cu(tpy)(\mathbf{1})]^{2+}$ subunits is electronically identical and they must be separated by a distance of at least 6 Å.[22] This spectrum is contrasted by that obtained for the charge neutral $[Cu(pda)(\mathbf{1})]_6$ oligopeptide, Figure 8B, in which the lines are broadened and the hyperfine coupling is reduced to $\sim 130 \times 10^{-4}$ cm^{-1}. These are consistent with weak interactions between Cu centers that give rise to some delocalization of the unpaired electrons. The spectra of the $[Cu(pda)(\mathbf{1})]_6$ is further complicated by the presence of (at least) a second set of peaks with lower intensity and similar $A_{||}$, which implies that several types of Cu complexes exist in this structure with slightly different electronic environments. For both the $[Cu(tpy)(\mathbf{1})]_6^{12+}$ and $[Cu(pda)(\mathbf{1})]_6$ hexapeptides, the values of $g_{||} > 2.1 > g_{\perp} > 2.0$ are typical for Cu complexes with a square planar geometry.[23]

The spectrum of the Cu-linked bpy trimer duplex (Figure 8C) is similar to that of the $[Cu(pda)(\mathbf{1})]_6$ hexapeptide, except that it is even further broadened and lacks hyperfine coupling. The

Figure 8. Frozen EPR spectra of 0.5 mM solutions of $[Cu(pda)(\mathbf{1})]_6$ (top), $[Cu(tpy)(\mathbf{1})]_6(ClO_4)_{12}$ (middle), and $[Cu(\mathbf{2})_2]_3(PF_6)_6$ (bottom).

(21) Lippard, S. J.; Berg, J. M. *Principles of Bioinorganic Chemistry*; University Science Books: California, 1994.
(22) Solomon, E. I.; Sundaram, U. M.; Machonkin, T. E. *Chem. Rev.* **1996**, *96*, 2563−2605.
(23) (a) Lucchesse, B.; Humphreys, K. J.; Lee, D.-H.; Incarvito, C. D.; Sommer, R. D.; Rheingold, A. L.; Karlin, K. D. *Inorg. Chem.* **2004**, *43*, 5987−5998. (b) Wei, N.; Murthy, N. N.; Karlin, K. D. *Inorg. Chem.* **1994**, *33*, 6093−6100.

Table 1. EPR Spectroscopy Parameters and Hyperfine Coupling Constants

complex	$g_{\|}$	$g_{\perp}$	$A_{\|} \times 10^{-4}$ (cm^{-1})
$[Cu(tpy)(\mathbf{1})]_6^{12+}$	2.28	2.06	167
$[Cu(pda)(\mathbf{1})]_6$	2.35	2.09	130
$[Cu(\mathbf{2})_2]_3^{6+}$		2.09	

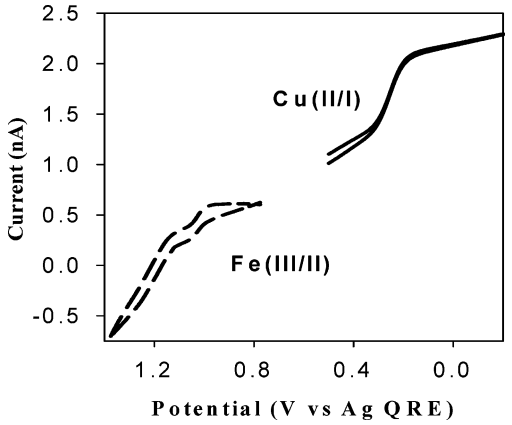

Figure 9. Cyclic voltammograms of $[Fe(\mathbf{2})_3]_2(ClO_4)_4$ and $[Cu(\mathbf{2})_2]_3(ClO_4)_6$, obtained using a 12.5 micron radius Pt working electrode at a scan rate of 5 mV/s, with backgrounds corrected for uncompensated resistance. Solutions contained 1 mM peptide duplex in acetonitrile.

overall shape is again consistent with a structure containing Cu atoms with several electronic environments. The lack of hyperfine peaks may be due to very small coupling constants but is most likely due to multiple Cu environments both within one molecule and between the isomeric forms that are present.

Taken together, the EPR spectra are consistent with the structures from molecular modeling in Figures 6 and 7. Based on these, $[Cu(pda)(\mathbf{1})]_6$ and $[Cu(\mathbf{2})_2]_3^{6+}$ would be expected to rotate polarized light because of their helical structures. However, our measurements of the molecules' circular dichroism spectra (see Supporting Information) did *not* contain evidence of optical activity for any of these multimetallic complexes. We rationalize this result based on the expected differences in the solution phase and frozen molecular structures of the single-strand peptide and note that the observation for the Cu-linked tripeptide duplex is again consistent with the presence of several geometric isomers.

Electrochemistry. The oligopeptide complexes and duplexes possess structural components (metal atoms and ligands), with unique oxidation and reduction properties. Each of the above oligopeptide sequences is expected to have a distinctive voltammetric signature based on the type and number of metal complex(es) linked to the peptide backbone. The voltammograms (not shown) of the py hexapeptides containing [Cu(pda)] and $[Cu(tpy)]^{2+}$ complexes are distinctive only in the large amount of adsorption to the electrode surface and extremely slow heterogeneous kinetics for the Cu(II/I) reduction (for both the tpy and pda complexes), which completely obfuscate further quantitative analysis.

Voltammetry of the Cu- and Fe-linked bpy oligopeptide duplexes is however quantitatively informative; Figure 9 contains voltammograms acquired with a microdisk electrode in acetonitrile solutions containing either the $[Fe(\mathbf{2})_3]_2^{4+}$ or $[Cu(\mathbf{2})_2]_3^{6+}$ bpy oligopeptide duplexes. Supporting electrolyte was *not* added to these solutions to avoid contamination of the very small quantities of available material with salt; therefore slow potential scan rates (5 mV/s) and compensation for solution resistance[24] were used to produce the voltammograms in Figure 9. In the case of the trimetallic Cu duplex, a sigmoidal wave attributed to the Cu(II/I) reduction was observed with a half wave potential of 0.22 V vs Ag QRE. Using the microelectrode limiting current at large overpotentials, and assuming that each of the three Cu atoms are reduced during the reaction, the diffusion coefficient of the Cu duplex is calculated to be 5×10^{-7} cm^2/s.[24]

The dimetallic Fe duplex exhibited a voltammetric response at more positive potentials, where the $[Fe(bpy)_3]^{3+/2+}$ oxidation is expected to appear. However in contrast to the Cu duplex, the Fe duplex voltammetry possesses an oxidative signature that appears to have two sequential reactions: the first of these is smaller and occurs at a half wave potential of 0.98 V and the second larger wave at 1.2 V vs Ag QRE. Background cyclic voltammograms of a nonmetalated peptide oligomer do not possess any redox activity within this potential region. The appearance of two waves is unusual and could arise from strong electronic interactions between the two metal centers or from the existence of two structural isomers of the $[Fe(\mathbf{2})_3]_2^{4+}$ duplex. The former of these has been ruled out because similar coupling in the Cu duplex (which is expected to be far more ordered) voltammetry is not observed and our molecular modeling predicts a substantial 1.1 nm separation between the Fe centers. Additionally, it would be expected that strong electronic coupling would result in two waves of equal magnitude in current: the wave observed at lower potentials is about half the size of the larger wave. We therefore believe that the two peaks in the voltammetry are a result of two isomeric forms of the Fe duplex that contain Fe complexes with different degrees of conformational stabilization, which is the subject of ongoing studies with larger quantities of duplex material.

Using the currents obtained for the Fe duplex, the diffusion coefficients for the waves at 0.98 and 1.2 V are determined[24] to be 5×10^{-7} and 1×10^{-6} cm^2/s, respectively. These values compare well with that calculated for the Cu duplex. In both cases, the solution phase diffusion coefficients are consistent with mass transport rates that are expected for structures of this size and charge.[25] The voltammetry therefore demonstrates that these relatively simple, homometallic oligopeptide duplexes have distinguishable electrochemical signatures.

Conclusions

We have synthesized two new artificial oligopeptides with pendant nitrogen-containing ligands and used these to prepare peptidic scaffolds that bind transition metal ions in a stoichiometric manner. In the case of the bpy oligomers, the metal ions cross-link the strands to self-assemble structures into double-stranded oligopeptide duplexes with sequence-dependent elec-

(24) Bard, A. J.; Faulkner, L. R. *Electrochemical Methods, Fundamentals and Applications*, 2nd ed.; John Wiley & Sons: New York, 2001.

(25) Compared to the diffusion coefficient of ferrocene (radius $\approx$ 2 Å) in acetonitrile ($\sim 10^{-5}$ cm^2/s) and using the voltammetrically determined diffusion coefficient (D), the Stokes−Einstein relationship ($D = k_BT/6\pi\eta r_H$) would predict a *hydrodynamic* radius (which would include stabilizing counterions and solvent molecules) for the metal-linked tripeptide duplexes of ~4 nm.

trochemical and spectroscopic properties. Our continuing efforts seek to obtain crystallographic confirmation of both the Fe^{2+} and Cu^{2+} duplex structures, to expand the library of artificial peptides, and to examine detailed optical and electronic properties of these supramolecular structures.

Acknowledgment. This work is dedicated to the memory of our friend and colleague R. Koerner. We gratefully acknowledge the Penn State Department of Chemistry NMR facility and especially Dr. Chris Falzone for assistance with 2-D NMR spectroscopy. This work was generously supported by a David and Lucile Packard Foundation Fellowship for Science and Engineering.

Supporting Information Available: High-resolution mass spectrometry data, circular dichroism and two-dimensional NMR spectra, with analysis. This material is available free of charge via the Internet at http://pubs.acs.org.

JA0510818